A Monolayer CDW-Mott Phase Robust Against Heat, Light and Doping

Angle-resolved photoemission spectroscopy showed that the band structure of a monolayer of the transition-metal dichalcogenide 1T-$TaSe_2$ is stable against heat, laser excitation and doping.

The combination of low-dimensionality and electron correlation are crucial for exotic quantum phenomena such as the Mott-insulating phase and high-temperature superconductivity. The transition-metal dichalcogenide (TMD) 1T-TaS_2 has attracted enormous interest because of its unique non-magnetic Mott-insulator nature, which is well known to be associated with a charge-density-wave (CDW) transition. In its bulk form, the CDW-Mott transition temperature $T_{CDW\text{-}Mott}$ for 1T-TaS_2 is, however, less than 200 K. Attempts to increase $T_{CDW\text{-}Mott}$ have not succeeded to date, but enhancement of $T_{CDW\text{-}Mott}$ is necessary for use in applications at room temperature and above. Researchers in an international collaboration have now shown that a monolayer of 1T-$TaSe_2$ exhibits a strong-coupling two-dimensional (2-D) CDW-Mott phase with transition temperature onset ~530 K. Furthermore, the electron-electron correlation-derived lower Hubbard band survives under external perturbations such as carrier doping and laser excitation, in contrast to the bulk counterpart.

The layered transition-metal dichalcogenide (TMD) 1T-TaS_2 is considered to be a special example of a bandwidth-controlled Mott-transition material[1,2] in the absence of magnetic order. Bulk 1T-TaS_2 undergoes a Mott transition accompanied by a commensurate CDW characterized by the star-of-David cluster (**Fig. 1(a)**) with a periodicity $\sqrt{13} \times \sqrt{13}$ (**Fig. 1(b)**), at $T_{CDW\text{-}Mott}$ ~200 K. Recent studies have focused on the exploration of unusual properties in the atomic-layer limit in TMD, with the possible emergence of exotic quantum phenomena in the pure 2D limit.[3] The nature of a pure 2D CDW-Mott phase in terms of its stability at high temperatures and under photoexcitation, possibility for magnetism, *etc.* compared with the 3D bulk case has been scarcely explored. Furthermore, the most important issue regarding the interplay between the Mott phase and dimensionality has yet to be clarified.

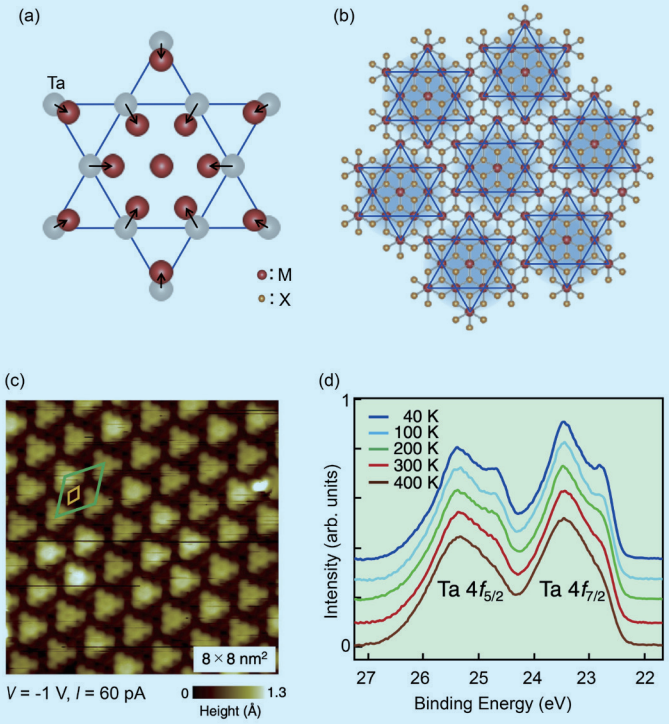

Fig. 1: Schematics of star-of-David clusters, scanning tunneling microscopy and core-level photoemission spectra of monolayer 1T-$TaSe_2$. (a) Schematics of displacement of Ta atoms in the star-of-David cluster. M and X represent transition-metal and chalcogen atoms, respectively. (b) Schematics of crystal structure for monolayer 1T-$TaSe_2$ and star-of-David clusters with periodicity $\sqrt{13} \times \sqrt{13}$. (c) STM image in surface area 8 × 8 nm^2 for monolayer 1T-$TaSe_2$ on bilayer graphene measured at T = 4.8 K. (d) Temperature dependence of EDCs around the Ta-4*f* core level measured with $h\nu$ = 260 eV for monolayer 1T-$TaSe_2$. [Reproduced from Ref. 4]

In this work, the authors grew high-quality single-phase monolayer 1T-$TaSe_2$ with a CDW-Mott transition temperature onset ~530 K. The samples were first characterized with a scanning tunneling microscope (**Fig. 1(c)**) to confirm the monolayer nature. Core-level photoemission spectra (**Fig. 1(d)**) showed a temperature-dependent splitting of the Ta 4*f* core levels, which is well known as a signature of CDW order in TMD materials. **Figure 2** (see next page) shows the temperature-dependent angle-resolved photoemission spectroscopy (ARPES) results that confirmed the CDW-Mott insulating phase to be stable up to high temperatures; the authors estimated a transition temperature $T_{CDW\text{-}Mott}$ ~530 K. The authors then carried out doping-dependent studies at beamline **TLS 21B1** of the Taiwan Light Source. A calibrated dosing of the monolayer 1T-$TaSe_2$ surface with K atoms was implemented; the corresponding ARPES spectra are shown in **Fig. 3** (see next page). The results showed that the lower Hubbard band, a characteristic of a strongly correlated CDW-Mott phase, survived with a large doping content and only shifted to higher binding energies,[4] as seen in **Fig. 3**.

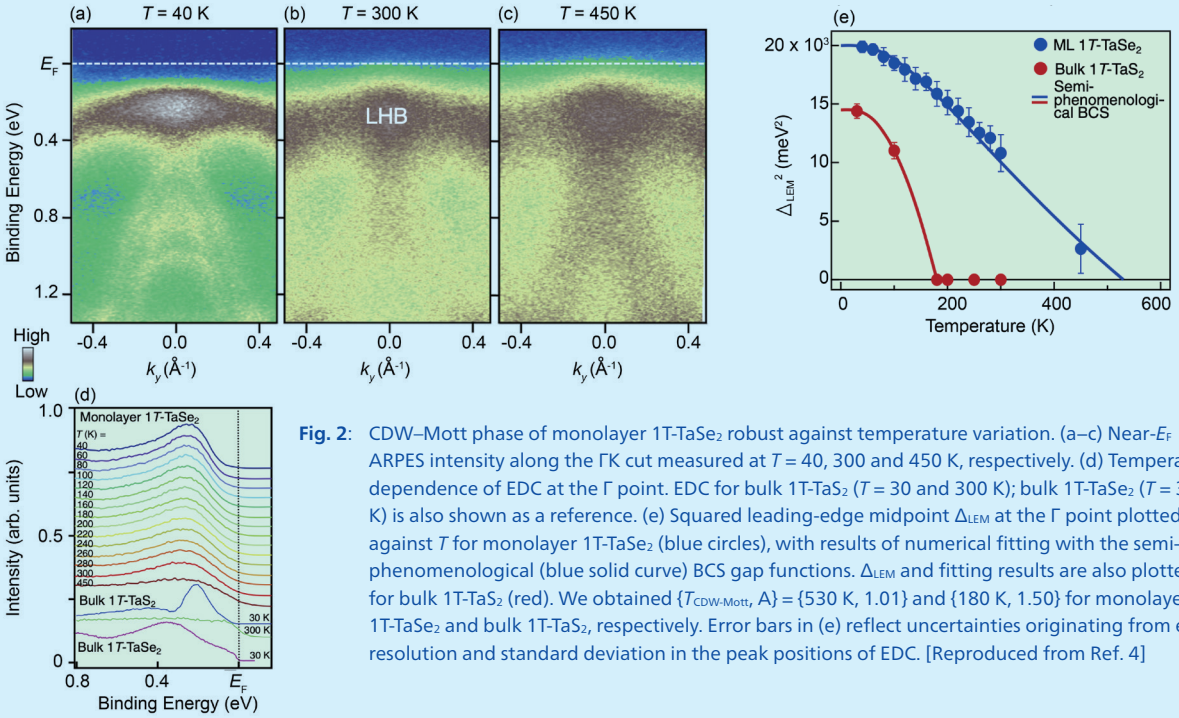

Fig. 2: CDW–Mott phase of monolayer 1T-$TaSe_2$ robust against temperature variation. (a–c) Near-E_F ARPES intensity along the ΓK cut measured at T = 40, 300 and 450 K, respectively. (d) Temperature dependence of EDC at the Γ point. EDC for bulk 1T-TaS_2 (T = 30 and 300 K); bulk 1T-$TaSe_2$ (T = 30 K) is also shown as a reference. (e) Squared leading-edge midpoint Δ_{LEM} at the Γ point plotted against T for monolayer 1T-$TaSe_2$ (blue circles), with results of numerical fitting with the semi-phenomenological (blue solid curve) BCS gap functions. Δ_{LEM} and fitting results are also plotted for bulk 1T-TaS_2 (red). We obtained $\{T_{CDW\text{-}Mott}, A\}$ = {530 K, 1.01} and {180 K, 1.50} for monolayer 1T-$TaSe_2$ and bulk 1T-TaS_2, respectively. Error bars in (e) reflect uncertainties originating from energy resolution and standard deviation in the peak positions of EDC. [Reproduced from Ref. 4]

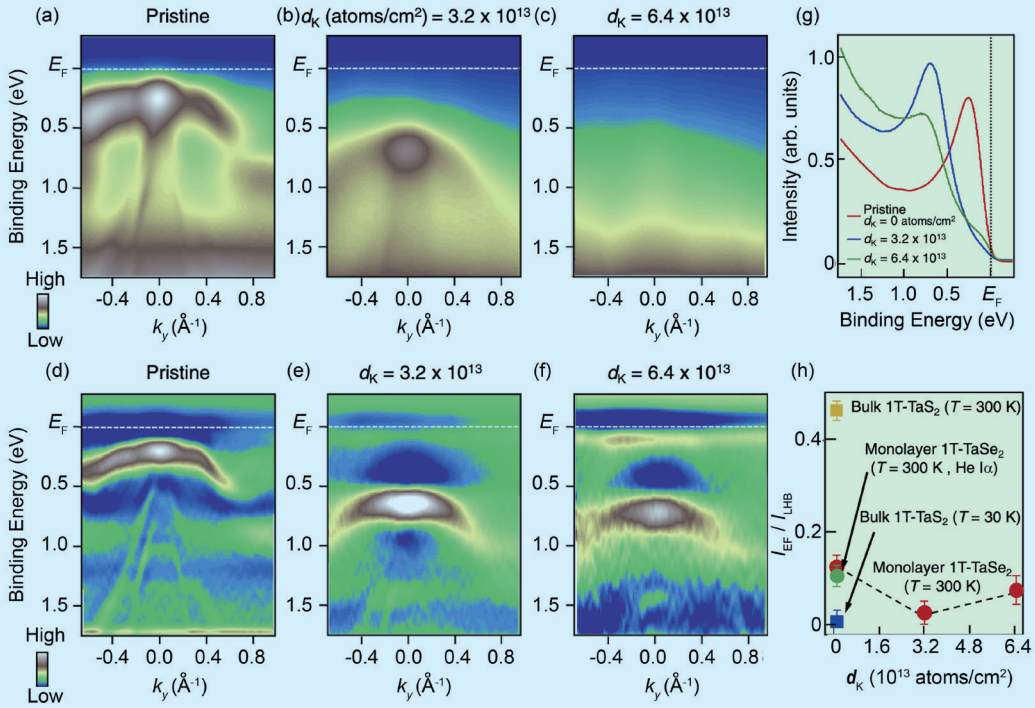

Fig. 3: CDW–Mott insulator phase in monolayer 1T-$TaSe_2$ robust against electron doping. (a–c) K-deposition dependence of ARPES intensity along the ΓK cut for monolayer 1T-$TaSe_2$ [potassium coverage d_K = 0 (pristine), 3.2 x 10^{13} and 6.4 x 10^{13} atoms/cm², respectively], measured at T = 300 K with $h\nu$ = 51 eV. (d–f) Same as (a–c), but obtained on taking the second derivative of EDC. (g) EDC at the Γ point for each d_K. (h) Plots of intensity at E_F with respect to that at LHB, I_{EF}/I_{LHB}, as a function of d_K, estimated from the EDC in (g). The I_{EF}/I_{LHB} values for bulk TaS_2 measured at T = 30 and 300 K are also plotted. Error bars reflect uncertainties originating from the energy resolution and statistics of data. [Reproduced from Ref. 4]

The authors further confirmed that the electronic band structure of the CDW-Mott phase was stable also under photoexcitation, using laser-based pump-probe ARPES measurements. From a careful analysis of all the data, the authors showed that the enhanced transition temperature, as well as the Mott-Hubbard and CDW gaps for monolayer 1T-$TaSe_2$, originate from (i) a lattice distortion in combination with enhanced electron-electron correlations, and (ii) a disappearance of interlayer hopping in the monolayer limit compared to the bulk. The study[4] thus established an effective method to

stabilize the CDW-Mott phase in terms of band engineering. The discovery of the robust CDW-Mott phase far above room temperature is considered valuable for developing practical CDW-Mott insulator-based ultrathin nanoelectronic devices. (Reported by Ashish Chainani)

This report features the work of Takafumi Sato, Katsuaki Sugawara and their collaborators published in Nat. Commun. ***12****, 5873 (2021).*

TLS 21B1 Angle-resolved UPS

- ARPES
- Materials Science, Condensed-matter Physics

References

1. P. Fazekas, E. Tosatti, Philos. Mag. B **39**, 229 (1979).
2. K. Rossnagel, N. V. Smith, Phys. Rev. B **73**, 073106 (2006).
3. K. S. Novoselov, D. Jiang, F. Schedin, T. J. Booth, V. V. Khotkevich, S. V. Morozov, A. K. Geim. PNAS **102**, 10451 (2005).
4. Y. Nakata, K. Sugawara, A. Chainani, H. Oka, C. Bao, S. Zhou, P.-Y. Chuang, C.-M. Cheng, T. Kawakami, Y. Saruta, T. Fukumura, S. Zhou, T. Takahashi, T. Sato, Nat. Commun. **12**, 5873 (2021).

A Route to Create Quantum Spin Hall Systems

A novel phenomenon termed the topological proximity effect, which occurs between a 2D material and a 3D topological insulator, has generated a paradigm that opens a route to create quantum spin Hall systems in monolayer-substrate heterostructures.

3D topological insulators (TI), which refer to the states of matter with an insulating gap in the bulk and gapless helical states on the surface, have attracted much attention due to their fascinating electronic structures. Proximity effects that occur in heterojunctions comprised of TIs and materials can provide an interesting platform to produce emerging quantum phenomena of Dirac fermions at the interfaces. For instance, it has been predicted that a hybrid structure made of a 3D TI and a superconductor can produce a superconducting proximity effect at the interface, which might lead to the emergence of 2D topological superconductivity hosting Majorana fermions. In graphene transferred on 3D TI, a strong proximity effect can induce opening of the band gap and strong spin-orbital coupling, which leads to a strong tunability and suppression of the spin signal and lifetime. Moreover, the predictions of such an interaction with non-topological states at the interface between a normal insulator (NT) and a TI might result in vertical twinning of the Dirac cone; the non-topological states can acquire a spin texture without magnetic doping. The study of the band structure of 2D NI/3D TI is significant to understand topological proximity effect; the results bear great potential for spintronics.

Herein, Jung-Chun Andrew Huang (National Cheng Kung University), Tay-Rong Chang (National Cheng Kung University), Cheng-Maw Cheng (NSRRC) and their teams studied a novel phenomenon termed a topological proximity effect, which occurs between a 2D material and a 3D TI. To understand further the change of electronic structure between Sb_2Te_3 and the antimonene/Sb_2Te_3 hybrid heterostructure, they performed an experiment at **TLS 21B1** beamline of the Taiwan Light Source recording angle-resolved photoemission spectra (ARPES) to probe the band structures. **Figures 1(a) and 1(b)** (see next page) show the band-mapping results of pristine Sb_2Te_3 and antimonene/Sb_2Te_3 recorded along the Γ-K direction. In a comparison of the two band-mapping results along direction Γ-K between Sb_2Te_3 and antimonene/Sb_2Te_3, an additional Sb-bilayer (BL)-derived band is observed near the Fermi level; the band structure of Sb_2Te_3 has a rigid band shift to larger binding energy. **Figure 1(c)** shows an enlargement of the energy scale in **Fig. 1(b)** to resolve the band dispersion around the Fermi level. The two Sb-BL-derived bands have an intersection at the Γ point near the Fermi level; a new Dirac point D_{sb} is located almost at the Fermi level. The observed band dispersion indicates that a new topological state has been formed in the antimonene/Sb_2Te_3 hybrid-heterostructure.

Figure 1(d) shows the calculated surface spectral weight with a color corresponding to the integrated charge